Semicond. Sci. Technol. **23** (2008) 075016 (7pp) doi:10.1088/0268-1242/23/7/075016

Properties of the ubiquitous p–n junction in semiconductor nanowires

M Zervos

Department of Mechanical Engineering-Materials Science Group, School Of Engineering, University of Cyprus, PO Box 20357, 75 Kallipoleos Avenue, Lefkosia 1678, Cyprus

E-mail: zervos@ucy.ac.cy

Received 20 February 2008, in final form 14 April 2008
Published 16 May 2008
Online at stacks.iop.org/SST/23/075016

Abstract

The properties of nanowires with built-in p–n junctions such as the energetic position of the one-dimensional sub-bands, charge distributions and band bending in equilibrium are determined by the self-consistent solution of the Poisson–Schrödinger equations in the effective mass approximation. The built-in potential V_{bi} of a GaAs nanowire with a radius of $R = 500$ Å and a symmetric built-in p–n junction are equal to $V_{bi} = 1.4$ V at $T = 300$ K, taking the donor and acceptor doping levels to be equal to $N_D = N_A = 1 \times 10^{18}$ cm^{-3}. The radial depletion is governed by the position of the conduction-band edge relative to the Fermi level at the surface, i.e. $e\phi_S = E_C - E_F$, and is a 'shell' with a thickness of 250 Å for $E_C - E_F = 0.7$ eV while the depletion width along z is $\approx$0.15 μm which is three times larger than the value of the bulk p–n junction taking the same doping level. It is found that decreasing the radius leads to a reduction in V_{bi} from 1.4 V at $R = 500$ Å to $V_{bi} = 0.02$ V at $R = 50$ Å and also complete depletion of the nanowire across its diameter and all along its length. Similarly, a reduction in the doping level leads to a decrease in V_{bi} down to $V_{bi} \approx 0.02$ V for $N_D = N_A = 1 \times 10^{16}$ cm^{-3} which is significantly lower than $V_{bi} \approx 1.1$ V obtained for the bulk p–n junction. These findings are discussed in a practical context related to growth and devices like nanowire solar cells.

1. Introduction

Semiconductor nanowires have been investigated extensively over the past few years and have been grown via the vapour–liquid–solid (VLS) mechanism using pulsed laser deposition [1], chemical vapour deposition [2] and molecular beam epitaxy [3]. Nanowires from not only group IV elements [4, 5], but also III–V [6–9] and II–VI [10] compound semiconductors have been realized, including variation of composition and doping along their length. Moreover, nanowire electronic and photonic devices, such as resonant tunnelling diodes [11], lasers [12], light emitting diodes [13], photodetectors [14] and solar cells [15], have been successfully demonstrated using individual nanowires (NWs). Most of these nanowire devices have a built-in p–n junction (pn-NWs) which is traditionally considered to be a fundamental device and building block in itself and exhibits rectifying current–voltage (I–V) characteristics. For instance, both Si pn-NWs with diameters down to 30 nm that were fabricated by Agarwal *et al* [16] and Ge pn-NWs with diameters of 60 nm that were grown by Tutuc *et al* [17] exhibit rectifying I–V characteristics.

Despite the large progress in the growth and fabrication of novel nanowire devices, less attention has been paid to the related device physics. Thus semiconductor pn-NWs have not been studied theoretically in much detail although as stated above, the p–n junction is considered to be a fundamental building block in itself. To be more specific, the only theoretical investigations of pn-NWs are those of Hu *et al* [18] and Kayes *et al* [19] who solved the Shockley–Poisson equations for pn-NWs without taking into account quantization. In particular, the charge distribution and depletion width in a Si nanowire that contains a single p–n junction along its length were determined by Hu *et al* [18] for radii, $R \leqslant 300$ nm, and doping levels between 1×10^{17} and 1×10^{18} cm^{-3}. The depletion width of the p–n junction was found to increase above the value of the bulk p–n junction as the nanowire radius was reduced below $R = 500$ Å. However, the built-in potential and its dependence on the doping level or the radius were not described. On the other hand, Kayes *et al* [19] investigated the properties of a nanowire with a p–n junction built in the radial direction by assuming that the electric field is zero outside the depletion region associated

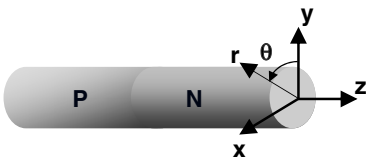

Figure 1. Schematic diagram of a nanowire with a built-in p–n junction in cylindrical coordinates r, z and θ.

with the p–n junction ignoring therefore any band bending at the nanowire surface. An important issue of course in nanowire device physics concerns the limits of classical drift-diffusion models [17] and in order to accurately determine the built-in potential and depletion width in pn-NWs it is necessary to take into account quantization and surface band bending.

In this work, the basic properties of a semiconductor nanowire that contains a single p–n junction along its length are determined via the self-consistent solution of the Poisson–Schrödinger equations in the effective mass approximation. The latter is valid for NWs with a radius greater than a few tens of nanometres and therefore applicable to a large number of NWs. The energetic position of the one-dimensional sub-bands, charge distribution, band bending and consequently the built-in potential and depletion width in such a pn-NW are determined in equilibrium. It is shown that the built-in potential drops with a decreasing radius or doping level well below the value of the built-in potential in a bulk p–n junction. In addition, it is shown that the thickness of the radial or surface depletion 'shell' that surrounds the conductive 'core' depends on the position of the conduction-band edge relative to the Fermi level at the surface which in turn governs the depletion along the length of the nanowire. These are critical aspects to be considered when tailoring the band profile of nanowires with built-in p–n junctions and are discussed in a practical context related to growth and p–n junction devices like nanowire solar cells.

2. Theory

As already stated above, we will consider the case of a nanowire that consists of two segments, i.e. an n-type and a p-type segment, as shown in figure 1 so that the effective mass m^*, permittivity ε_r and the energy gap E_G do not depend on r, z and θ respectively.

For the sake of simplicity, we consider the case of a symmetric built-in p–n junction so we will take the acceptor and donor doping densities to be equal on either side of the p–n junction, i.e. $N_A = N_D$. In the case of an infinitely long pn-NW, electrons are free along z but are confined in r and θ on the n side and therefore occupy one-dimensional sub-bands in the conduction band (CB) forming a one-dimensional electron gas (1DEG). On the other hand, holes on the p side occupy one-dimensional sub-bands in the valence band (VB) and form a one-dimensional hole gas (1DHG). To begin with, the energetic position of the one-dimensional sub-bands, charge distribution and band bending will be determined by the self-consistent solution of Poisson–Schrödinger's equations in r and θ for the infinitely long n- and p-type segments separately. This is necessary to set up and verify the three-dimensional, self-consistent calculation of the finite length pn-NW.

In a self-consistent Poisson–Schrödinger (SCPS) calculation, Schrödinger's equation is initially solved for a trial potential V and the charge distribution ρ is subsequently determined by multiplying the normalized probability density, $|\psi_k|^2$, by the thermal occupancy of each sub-band with energy E_k using Fermi–Dirac statistics and summing over all k. The Poisson equation is then solved for this charge distribution in order to find a new potential V' and the process is repeated until convergence is reached. We first consider the case of an infinitely long n-type nanowire and begin with Schrödinger's equation in r and θ, which is given by

$$-\frac{\hbar^2}{2}\left[\frac{\partial}{\partial r}\frac{1}{m^*}\frac{\partial\psi}{\partial r}+\frac{1}{r}\frac{1}{m^*}\frac{\partial\psi}{\partial r}+\frac{1}{r^2}\frac{\partial}{\partial\theta}\frac{1}{m^*}\frac{\partial\psi}{\partial\theta}\right]+V\psi=E\psi, \tag{1}$$

where $\hbar$ is Planck's constant divided by 2π, $m^*(r,\theta)$ is the effective mass of the electron, $V(r,\theta)$ is the conduction-band edge potential, $\psi(r,\theta)$ is the electron wavefunction and E is the corresponding energy. We assume that the potential is circularly symmetric and hence we consider wavefunctions of the form $\psi(r,\theta)=\psi(r)\,\mathrm{e}^{\mathrm{i}m\theta}$, where $m=0,\pm1,\pm2,\pm3,\ldots$ is the angular momentum quantum number corresponding to quantization in θ. Finite differences are used to express Schrödinger's equation into a standard matrix eigenvalue problem, i.e.

$$H_m\Psi_m=E_m\Psi_m, \tag{2}$$

where H_m is the Hamiltonian matrix for a specific angular momentum number m, which has been described in detail elsewhere [20]. In the case of an infinitely long nanowire, the wavefunctions take the form $\psi(r,z,\theta)=\psi(r)\,\mathrm{e}^{\mathrm{i}m\theta}\,\mathrm{e}^{\mathrm{i}lz}$ and are normalized according to

$$(2\pi)^2\int_0^R r|\Psi(r)|^2\,\mathrm{d}r=1, \tag{3}$$

where R is the radius of the nanowire and one factor of 2π is due to integration with respect to θ while the other factor of 2π is due to the normalization of the plane waves in the z-direction. The one-dimensional electron gas (1DEG) density is given by the expression

$$n_{1\mathrm{DEG}}(r)=\sum\nolimits_k n_k|\Psi_k(r)|^2, \tag{4}$$

where summation runs over the sub-bands and for each k the angular momentum quantum number takes on the values $m=0,\pm1,\pm2,\pm3,\ldots$. Furthermore, n_k is the thermal occupancy of the kth sub-band which is given by

$$n_k=\frac{1}{\pi}\sqrt{\frac{2m^*k_\mathrm{B}T}{\hbar^2}}\,\Im_{-1/2}\left(\frac{E_\mathrm{F}-E_k}{k_\mathrm{B}T}\right), \tag{5}$$

where k_B is Boltzmann's constant, T is the temperature, E_F is the Fermi level, E_k is the energy of the bottom of the kth sub-band and $\Im_{-1/2}$ is the Fermi–Dirac integral of order $-1/2$. The factor in front of $\Im_{-1/2}$ comes from the 1D density of states (DOS) and the units of n_k are those of a line density (m^{-1}), which when multiplied by the normalized probability density

gives the volume density $n_{1DEG}(r)$. The overall charge density $\rho(r)$ is then given by

$$\rho(r) = e\big(N_D^+(r) - n_{1DEG}(r)\big), \tag{6}$$

where e is the electron charge and $N_D^+(r)$ is the distribution of the ionized donor impurities. Using $\rho(r)$ and the potential $V(r)$ which is related to the electrostatic potential $\phi(r)$ via $V(r) = -e\phi(r)$, it is possible to solve the Poisson equation in cylindrical coordinates:

$$\frac{\partial^2\phi}{\partial r^2} + \frac{1}{r}\frac{\partial\phi}{\partial r} = -\frac{\rho(r)}{\varepsilon_o\varepsilon_r}, \tag{7}$$

where ε_o is the permittivity of the free space and ε_r is the relative permittivity. The exact or self-consistent potential $\phi_0(r)$ is expressed in terms of the trial potential $\phi(r)$ and a correction potential $\delta\phi(r)$:

$$\phi_o(r) = \phi(r) + \delta\phi(r). \tag{8}$$

This is substituted into Poisson's equation which is solved to find $\delta\phi(r)$ so as to iterate until convergence is reached. However, it is necessary to find an expression for the change in the quantum density $n_{1DEG}(r)$ given a small change $\delta\phi$. This is required since $n_{1DEG}(r)$ is also dependent on the potential ϕ, i.e. $n_{1DEG}(r, \phi)$. A perturbation $\phi \to \phi + \delta\phi$ will change the quantum electron density from $n_{1DEG}(\phi)$ to $n_{1DEG}(\phi + \delta\phi)$:

$$n_{1DEG}(\phi + \delta\phi) = n_{1DEG}(\phi) + \delta n_{1DEG}(\phi, \delta\phi). \tag{9}$$

The approach of Trellakis *et al* [21] is adopted, who derives an expression for $\delta n_{1DEG}(\phi, \delta\phi)$ applicable to quantization in an infinite quantum wire of a square cross-section and then using the derivative property of the Fermi–Dirac integrals simplifies $n_{1DEG}(\phi + \delta\phi)$ to

$$n_{1DEG}(\phi + \delta\phi) = \frac{1}{\pi}\sqrt{\frac{2m^*k_BT}{\hbar^2}} \times \sum_k \psi_k^2(\phi)\Im_{-3/2}\left(\frac{E_F - E_k + q\delta\phi}{k_BT}\right). \tag{10}$$

Inserting $n_{1DEG}(\phi + \delta\phi)$ given by equation (10) into the Poisson equation yields an expression that may be expressed in a matrix form and is effectively a linear system of equations in the unknown vector $\delta\phi$. After adding $\delta\phi(r, z)$ onto the trial potential $\phi(r, z)$, the process of solving the Poisson–Schrödinger equations is repeated until convergence is reached, i.e. when the average correction potential $\overline{\delta\phi}$ is typically less than 0.1 meV and charge neutrality is achieved.

In the case of the infinitely long p-type nanowire, the energetic position of the one-dimensional sub-bands, charge distributions and band bending in the valence band are determined by solving Schrödinger's equation in r and θ as described above, first for the heavy hole and then for light holes, taking into account the valence-band edge potential profile along r, i.e. $E_{VB} = E_{CB} - E_G$, which is inverted in order to use equations (1)–(10) by changing n → p, $E_C \to E_V$, 1DEG → 1DHG and $N_D^+ \to N_A^-$. The self-consistent valence-band profile along r obtained in this way is reliable for the radii and doping levels considered in this work. A full band-structure calculation on the other hand is mandatory for nanowires that have radii of the order of a few nanometres [24, 25].

Having obtained the SC band profile for the infinitely long, n- and p-type nanowires, it is possible to determine in a simple way the built-in potential of the pn-NW formed by joining the two, simply by taking into account (i) the position of the conduction-band (CB) edge E_C with respect to the Fermi level E_F at the core of the infinitely long n-type nanowire, i.e. $(E_C - E_F)_N^\infty$, (ii) the position of the valence-band (VB) edge E_V with respect to the Fermi level E_F at the core of the infinitely long p-type nanowire, i.e. $(E_F - E_V)_P^\infty$, and (iii) using

$$eV_{bi} = E_G - (E_C - E_F)_N^\infty - (E_F - E_V)_P^\infty. \tag{11}$$

This is in direct analogy with the calculation of the built-in potential for the planar p–n junction, but it must be clear that the value of V_{bi} obtained this way for the pn-NW is actually the maximum of the three-dimensional, built-in potential barrier landscape which occurs along z at the core of the nanowire. More importantly, $(E_C - E_F)_N^\infty$ and $(E_F - E_V)_P^\infty$ determined from the self-consistent calculations of the n- and p-type nanowires are important to know in order to ensure that the potential landscape converges correctly at the ends of the nanowire, far away from the p–n junction in the three-dimensional (3D) SCPS calculation of the pn-NW which is used as a criterion to set the length of the NW.

Now in order to determine the electronic properties of the finite length pn-NW shown in figure 1, it is necessary to carry out a mixed-type 3D-SCPS calculation in r, z and θ which involves electrons (e) and holes (h). The 3D-SCPS calculation of the 'quasi' one-dimensional charge distributions including the conduction- and valence-band potential landscapes in such a pn-NW is based on an older 3D-SCPS solver [20] that was developed for nanowires with built-in barriers and quantum dots, otherwise known as one-dimensional heterostructures [11] and is extended here to include holes. We will briefly describe the 3D-SCPS solver beginning with Schrödinger's equation in r, z and θ:

$$-\frac{\hbar^2}{2}\left[\frac{\partial}{\partial r}\frac{1}{m^*}\frac{\partial\psi}{\partial r} + \frac{1}{r}\frac{1}{m^*}\frac{\partial\psi}{\partial r} + \frac{\partial}{\partial z}\frac{1}{m^*}\frac{\partial\psi}{\partial z} + \frac{1}{r^2}\frac{\partial}{\partial\theta}\frac{1}{m^*}\frac{\partial\psi}{\partial\theta}\right] + V\psi = E\psi, \tag{12}$$

where V and ψ are now dependent also on z, i.e. $V(r, z)$ and $\psi(r, z, \theta)$. We again assume that the potential is circularly symmetric so that the wavefunctions that have the form $\psi(r, z, \theta) = \psi(r, z)\,e^{im\theta}$. Finite differences were used to express Schrödinger's equation into a standard matrix eigenvalue problem [20], which is solved first for electrons in the conduction band and then holes in the valence-band. This yields the energies and wavefunctions of discrete electron states on the n-type side and discrete hole states in the p-type side. Since we are dealing with a finite length pn-NW, the wavefunctions are normalized according to

$$\int_0^L dz \int_0^R 2\pi r|\Psi(r, z)|^2\,dr = 1. \tag{13}$$

Here, L is the length of the nanowire. Note that while the wavefunctions are circularly symmetric in θ, they decay not only along r but also along z in the vicinity of the built-in barrier associated with the p–n junction. The corresponding 'quasi' one-dimensional charge distributions in the n- and p-type segments are simply determined by multiplying the

thermal occupancy of each state by 2 for spin up and spin down and then by the normalized probability density and summing over all states k. Thus for electrons on the n side of the pn-NW, the charge distribution n' is given by

$$n'(r, z) = 2\sum_k |\Psi_k(r, z)|^2 \frac{1}{1 + e^{(E_k - E_F)/k_B T}} \tag{14}$$

with a similar expression for p'. In order to obtain rapid convergence and a flat-band condition at the ends of the pn-NW along the z-direction, it is necessary to calculate the 1DEG charge distribution at the end of the nanowire on the n side by solving equations (1)–(4), similarly for the 1DHG on the p side. This is exactly analogous to the calculation of the three-dimensional charge distribution in the buffer layer of a two-dimensional electron gas (2DEG) quantum well heterostructure. The overall charge density $\rho(r, z)$ is then given by

$$\rho(r, z) = e\big(N_D^+(r, z) - n'(r, z) + p'(r, z) - N_A^-(r, z)\big), \tag{15}$$

where $n'(r, z)$ and $p'(r, z)$ now include the charge densities evaluated at the ends of the nanowire. Using $\rho(r, z)$ and the potential $V(r, z)$ which is related to the electrostatic potential $\phi(r, z)$ via $V(r, z) = -e\phi(r, z)$, it is possible to solve Poisson's equation in r and z:

$$\frac{\partial^2\phi}{\partial r^2} + \frac{1}{r}\frac{\partial\phi}{\partial r} + \frac{\partial^2\phi}{\partial z^2} = -\frac{\rho(r, z)}{\varepsilon_o\varepsilon_r}. \tag{16}$$

The exact or self-consistent potential $\phi_0(r, z)$ is expressed again in terms of a trial potential $\phi(r, z)$ and a correction potential $\delta\phi(r, z)$, i.e.

$$\phi_o(r, z) = \phi(r, z) + \delta\phi(r, z). \tag{17}$$

This is substituted into Poisson's equation which is solved to find $\delta\phi(r)$. However, it is again necessary to find an expression for the change in the quantum density $n'(r, z; \phi)$ and $p'(r, z; \phi)$ for a small change $\delta\phi$ since they are functionally dependent on the potential ϕ. A perturbation $\phi \to \phi + \delta\phi$ will change the quantum electron density from $n'(\phi)$ to $n'(\phi + \delta\phi)$:

$$n'(\phi + \delta\phi) = n'(\phi) + \delta n'(\phi, \delta\phi). \tag{18}$$

It was shown [20] that for full quantization in a finite length nanowire, $\delta n'(\phi, \delta\phi)$ is given by

$$\delta n'(\phi, \delta\phi) = -2e\sum_k |\psi_k(\phi)|^2 \Im'(E_k)\delta\phi. \tag{19}$$

Inserting $\delta n'(\phi, \delta\phi)$ into the expression for $n'(\phi + \delta\phi)$ given by (18) and using the latter in the Poisson equation yields an expression that may be cast in a matrix form and is a linear system of equations in the unknown $\delta\phi$. Note that the validity of the matrix set-up was checked and verified against the analytical solution of the Laplace equation for a cylinder of length L and radius R containing zero charge in its interior and having a potential equal to V on the top side, i.e. $z = L$ and zero potential on the side $r = R$ and bottom face, i.e. $z = 0$ [20]. After solving for $\delta\phi(r, z)$, this is added onto the trial potential $\phi(r, z)$ and the process of solving the Schrödinger–Poisson equations is repeated until convergence is reached.

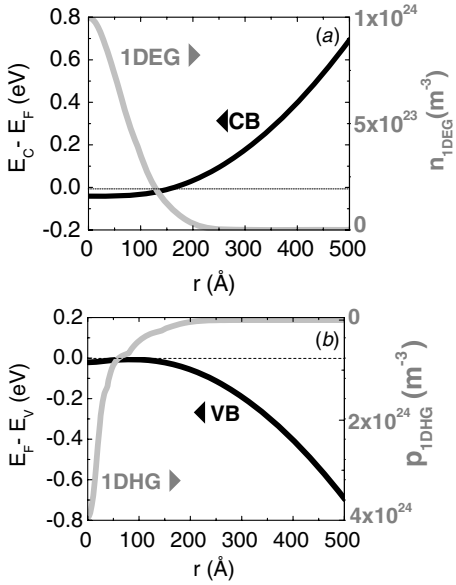

Figure 2. (*a*) SCPS CB edge potential profile with respect to the Fermi level, i.e. $E_C - E_F$ along r, in an n-type GaAs nanowire with a uniform ionized donor density of $N_D^+ = 1 \times 10^{18}$ cm^{-3} at $T =$ 300 K and $e\phi_S = E_C - E_F = 0.7$ eV at the surface. Also shown is the 1DEG distribution which has a line density of 3×10^8 m^{-1}. (*b*) SCPS VB edge potential profile relative to the Fermi level, i.e. $E_F - E_V$ along r, in a p-type GaAs nanowire with a uniform ionized acceptor density of $N_A^- = 1 \times 10^{18}$ cm^{-3} at $T = 300$ K and $e\phi_S = E_F - E_V = -0.7$ eV at the surface. The band bending is opposite to that shown in (*a*) and the 1DHG distribution has been inverted in order to make clear its position relative to the potential.

3. Results and discussion

The self-consistent band profile of an infinitely long n-type GaAs nanowire that has a radius of $R = 500$ Å and a uniform donor impurity distribution with a density of $N_D = 1 \times 10^{18}$ cm^{-3} is shown in figure 2(*a*) where in analogy with Leonard and Talin [22], the Fermi level was taken to be at the middle of the gap for GaAs, i.e. $e\phi_S = E_C - E_F = 0.7$ eV at the surface. There are two one-dimensional sub-bands below the Fermi level at $E_0 = -27$ meV and $E_1 = -9$ meV corresponding to the lowest sub-bands of $m = 0$ and $m = 1$ ladder of states respectively. Both sub-bands are above the conduction-band edge which resides ≈40 meV below the Fermi level at the core of the nanowire and they are occupied by electrons which form a 1DEG, which is also shown in figure 2(*a*). The 1DEG distribution has a maximum at the core of the nanowire and diminishes to zero at $r \approx 250$ Å. In addition, the electric field is zero in the radial direction at the core of the nanowire, i.e. $r = 0$ Å, corresponding to the desired flat-band boundary condition.

On the other hand, the self-consistent band profile of an infinitely long p-type GaAs nanowire with a radius of $R =$ 500 Å and a uniform acceptor impurity distribution with a density of $N_A = 1 \times 10^{18}$ cm^{-3} is shown in figure 2(*b*) again taking $e\phi_S = E_C - E_F = 0.7$ eV. Recall that increasing energy for holes is downwards in figure 2(*b*). The lowest heavy-hole sub-band is situated at $E_0 = -0.4$ meV and is therefore very

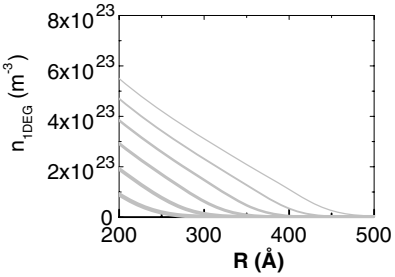

Figure 3. The dependence of the 1DEG charge density and distribution on the position of the conduction-band edge relative to the Fermi level at the surface, i.e. $e\phi_S = E_C - E_F$ in an n-type GaAs nanowire taking $N_D = 1 \times 10^{18}$ cm^{-3} and $T = 300$ K. The value of $e\phi_S$ is varied between 0.1 eV, for the highest 1DEG charge density line, and 0.6 eV, in increments of 0.1 eV.

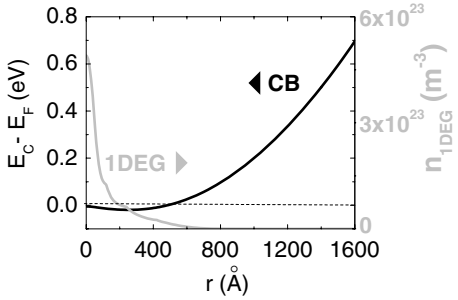

Figure 4. SCPS, CB edge potential profile along r in an n-type GaAs nanowire with $R = 1600$ Å, a uniform ionized donor density of $N_D^+ = 1 \times 10^{17}$ cm^{-3} at $T = 300$ K and $e\phi_S = E_C - E_F = 0.7$ eV. Also shown is the 1DEG distribution, with a line density of 4×10^8 m^{-1}, which decays to zero half-way along r.

close to the valence-band edge which coincides more or less with the Fermi level at the core of the nanowire. In contrast, the light-hole sub-bands are not occupied heavily and do not contribute towards the band bending in the radial direction. The overall 1DHG distribution which is shown inverted for convenience in figure 2(*b*) has a maximum at the core and diminishes to zero at $r \approx 250$ Å. From the self-consistent band profiles of the n- and p-type nanowires shown in figures 2(*a*) and (*b*), it is evident that the surface depletion is a 'shell' that surrounds the conductive 'core' of the nanowire. The one-dimensional charge is distributed within the 'core' and diminishes to zero approximately half-way along the radius in figures 2(*a*) and (*b*) due to the surface depletion. As we shall see shortly, the extent of the surface depletion depends on the position of the conduction-band edge relative to the Fermi level at the surface of the nanowire, i.e. $e\phi_S = E_C - E_F$. Therefore, the physical and chemical properties of the surface must be carefully controlled during or after growth in order to control the value of $e\phi_S$ [22, 23], which in turn controls the one-dimensional charge distribution and density. The dependence of the charge distribution and radial depletion thickness on $e\phi_S = E_C - E_F$ is shown in figure 3 for an infinitely long n-type GaAs nanowire with $R = 500$ Å and $N_D = 1 \times 10^{18}$ cm^{-3}. Decreasing the surface potential $e\phi_S = E_C - E_F$ leads to a reduction in the thickness of the surface depletion shell, an increase in the peak 1DEG density at the core of the nanowire and an extension of the charge distribution tail towards the surface. For $e\phi_S = 0.7$ eV, the charge distribution diminishes to zero about half-way along the radius, i.e. at $r \approx 250$ Å, but upon reducing $e\phi_S \to 0.1$ eV the tail of the 1DEG extends to $r = 450$ Å. For a given radius and doping level, the band bending along the radial direction in an n- or p-type nanowire will lead to a U-shaped potential across its diameter and the one-dimensional sub-bands will be occupied depending on $e\phi_S = E_C - E_F$. For small radii and realistic doping levels in the range 1×10^{16}–1×10^{18} cm^{-3}, it is necessary to have $e\phi_S = E_C - E_F \ll 0.7$ eV in order to obtain a reasonable one-dimensional charge density, else the nanowire will be depleted right across its diameter and along its entire length. For larger radii, $e\phi_S = E_C - E_F$ cannot be ignored, even in the case of nanowires with diameters of a few hundreds of nanometres. To be specific, a GaAs nanowire with $R = 1600$ Å and $N_D = 1 \times 10^{17}$ cm^{-3} has a substantial radial or surface depletion thickness of 800 Å as shown in figure 4, for $e\phi_S = E_C - E_F = 0.7$ eV. Note that the 1DEG line density has increased by 1×10^8 m^{-1} compared to the GaAs NW with $R = 500$ Å and $N_A = N_D = 1 \times 10^{18}$ cm^{-3} due to the larger volume although the doping level is an order of magnitude smaller.

Control of $e\phi_S = E_C - E_F$ is therefore essential for tailoring the 1DEG density and distribution but also to avoid the formation of unwanted depleted and conductive segments in series, i.e. essentially quantum dots, which may complicate or even obscure device operation. So far we considered the n- and p-type nanowires in isolation. If one 'joins' them, it is easy to determine the built-in barrier height at the p–n junction using equation (10). In the case of a GaAs pn-NW with $R = 500$ Å and $N_A = N_D = 1 \times 10^{18}$ cm^{-3}, we obtain $V_{bi} \approx 1.4$ V and this is as expected very close to the band-gap of GaAs, i.e. $E_G = 1.42$ eV at $T = 300$ K due to the fact that a degenerate one-dimensional electron and hole gas exists on either side of the p–n junction.

However, it is not possible to determine the extent of the depletion along z in the vicinity of the p–n junction by 'joining' the n- and p-type segments. It is therefore necessary to consider the self-consistent, three-dimensional, built-in potential landscape for the GaAs pn-NW which is shown in figure 5(*a*). The built-in potential barrier in the vicinity of the p–n junction has a maximum height of 1.4 eV along z at $r = 0$ Å in agreement with the value obtained above. Note that the electric field far away from the p–n junction along z is zero corresponding to the desired flat-band condition. The depletion width along z in the vicinity of the p–n junction is ≈ 0.15 μm, and a cutaway of the three-dimensional potential landscape along z and $r = 0$ Å is shown in figure 5(*b*). This depletion width is about three times larger than that of a bulk p–n junction which is equal to 0.05 μm taking $N_A = N_D = 1 \times 10^{18}$ cm^{-3} and actually depends on the thickness of the surface depletion 'shell' which as explained above extends along the entire length of the nanowire and is governed by $e\phi_S = E_C - E_F$. An increase in the radius will have a direct effect on the depletion width along z in the vicinity of the p–n junction which will converge towards the bulk p–n junction value. However, a reduction in the radius

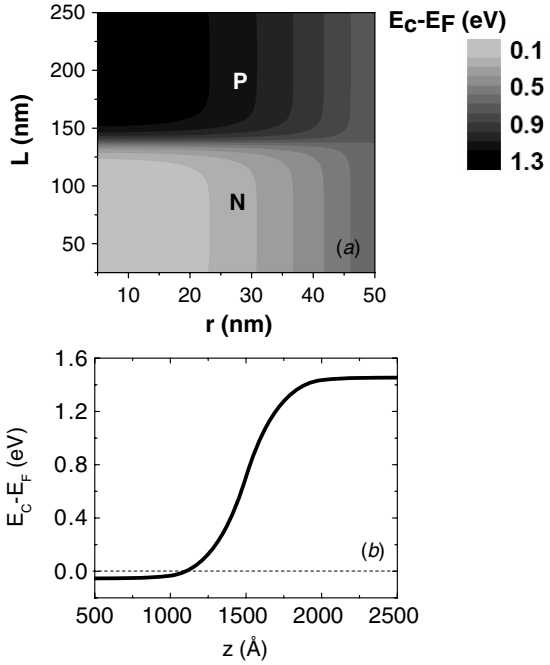

Figure 5. (*a*) 3D-SCPS CB edge potential landscape with respect to the Fermi level along r and z in a GaAs nanowire with a symmetric built-in p–n junction and $N_D^+ = N_A^- = 1 \times 10^{18}$ cm^{-3} at $T =$ 300 K. (*b*) Cutaway of the 3D-SCPS CB edge potential landscape shown in (*a*) along z at $r = 0$ Å.

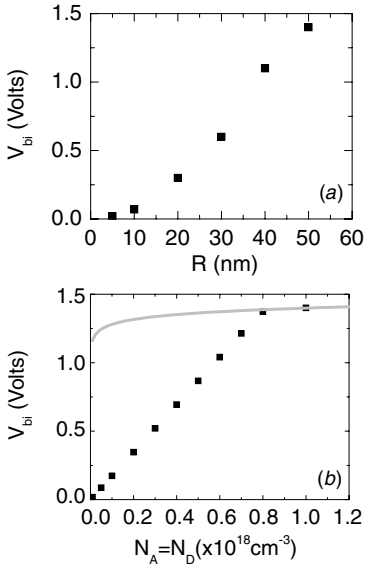

Figure 6. The dependence of the built-in potential V_{bi} on (*a*) the radius and (*b*) doping level in a GaAs pn-NW with $R = 500$ Å, $e\phi_S = E_C - E_F = 0.7$ eV and $T = 300$ K. The solid line in (*b*) corresponds to the 'bulk' p–n junction.

simply translates into a lower number of donor and acceptor impurities in the n- and p-type segments respectively which do not induce sufficient band bending in the r- and z-directions resulting into a decreasing built-in potential barrier height and increased depletion. To be specific, the built-in potential drops from $V_{bi} \approx 1.4$ V for a pn-NW with $R = 500$ Å down to $V_{bi} \approx 0.02$ eV for $R = 50$ Å as shown in figure 6(*a*) for a pn-NW with $N_A = N_D = 1 \times 10^{18}$ cm^{-3} and $e\phi_S = E_C - E_F =$ 0.7 eV. Moreover, the depletion extends right across the diameter and all along the length of the pn-NW for $R < 500$ Å. Thus for radii $R < 500$ Å, the properties of the p–n junction are drastically different compared to those of a bulk p–n junction and this value of the radius is in agreement with Hu *et al* [18] who find that the p–n junction properties take on values that are 'bulk' like for $R > 500$ Å irrespective of the doping level.

Achieving a high built-in potential and a reasonable charge distribution in pn-NWs with $R < 500$ Å requires n- and p-type doping levels that are well in excess of 1×10^{18} cm^{-3} taking $e\phi_S = E_C - E_F = 0.7$ eV, which may not be straightforward to achieve in nanowires.

Similar to its dependence on the radius, the built-in potential drops with a decreasing doping level in the pn-NW with $R = 500$ Å, as shown in figure 6(*b*), and shows a markedly different dependence on the doping level compared to the bulk p–n junction. A reduction in the doping level leads to a decrease in the built-in potential from $V_{bi} \approx 1.4$ V down to $V_{bi} \approx 0.02$ V in a GaAs pn-NW with $R = 500$ Å and $N_D = N_A = 1 \times 10^{16}$ cm^{-3} which is significantly lower than $V_{bi} \approx$ 1.1 V obtained in the bulk p–n junction using the same doping levels. From the above, it is evident that controlling the radius, doping levels and surface potential is critical to tailoring the band profile of nanowires with built-in p–n junctions. This is particularly difficult to do in nanowires with radii of the order of a few nanometres to a few tens of nanometres since large doping levels are required to induce sufficient band bending. High doping levels are difficult to achieve because n- and p-type impurities are incorporated during growth along the entire length of the nanowires and special procedures must be applied to achieve pn-NWs [18]. However, doping requirements may be relaxed by growing nanowires with diameters equal to a few hundreds of nanometres. As shown in figure 4, an n-type GaAs NW with $R = 1600$ Å and $N_D = 1 \times 10^{17}$ cm^{-3} has a radial or surface depletion thickness of 800 Å taking $e\phi_S = E_C - E_F = 0.7$ eV, while the one-dimensional charge density is actually higher compared to the pn-NW with $R = 500$ Å and $N_D = 1 \times 10^{18}$ cm^{-3}. The radial depletion thickness is ≈800 Å, i.e. three times larger than the depletion in the pn-NW with a radius of $R = 500$ Å, but still extends half-way along the radius R.

High 'core' carrier densities are desirable in pn-NW devices in order to reduce the series resistance of the n- and p-type segments which may be critical for certain applications, e.g. nanowire solar cells (NWSCs), since the short circuit current (I_{SC}) of individual nanowires is of the order of a few hundreds of pA as shown recently in a Si NW with a p–i–n junction built in the radial direction [15]. A large series resistance would lead to a drastic reduction in I_{SC} and a concomitant drop in the maximum power and efficiency, and this would also apply to NWSCs based on pn-NWs like those shown in figure 1. Therefore, pn-NWs with diameters equal to a few hundreds of nanometres, hereafter called 'fat' NWs, are preferable for NWSCs.

Moreover, large depletion regions are desirable in pn-NWs used in NWSCs in order to increase the short circuit current which is directly proportional to the depletion volume dV, i.e. $I_{SC} = e(G \times dV)$, where G is the generation rate. In the case of a radial pn-NW, the depletion associated with the p–n junction extends along the entire length of the nanowire and therefore I_{SC} scales linearly with the length L. The radial depletion of the p–n junction is larger in 'fat' NWs especially when the doping level is reduced, therefore justifying their use in NWSCs. However, although radial pn-NWs are suitable for NWSCs, it is necessary to contact separately the n shell and p-type core which implies elaborate processing that may compromise the cost benefit of third-generation NWSCs. In the case of the pn-NW shown in figure 1, the depletion associated with the p–n junction that extends along z is not dependent on the length L. However, incident photons will be absorbed and create electron–hole pairs in the surface depletion 'shell' which extends along the entire length of the pn-NW. Carriers generated in the surface depletion will separate along r and may contribute towards the short circuit current, and in fact this will also occur in a radial pn-NW. The larger one-dimensional charge densities and extended depletions that may be realized in pn-NWs with diameters of a few hundreds of nanometres using moderate doping levels make band-profile tailoring of pn-NW devices much more feasible at the cost of losing the benefits of quantization and band-gap adjustment that is possible in NWs with diameters of a few nanometres to a few tens of nanometres.

4. Conclusions

In conclusion, the basic properties of pn-NWs like the built-in potential and depletion width associated with the p–n junction have been determined by the self-consistent solution of the Poisson–Schrödinger equations in the effective mass approximation and cylindrical coordinates. The built-in potential of a GaAs pn-NW with a radius of $R = 500$ Å and a symmetric, built-in p–n junction is equal to $V_{bi} = 1.4$ V at $T = 300$ K, taking doping levels equal to $N_D = N_A = 1 \times 10^{18}$ cm^{-3}. The radial or surface depletion is governed by the position of the conduction-band edge relative to the Fermi level at the surface, and this in turn controls the depletion length along z which is larger than the corresponding value of the bulk p–n junction. Decreasing the radius below $R = 500$ Å leads to a significant reduction in the built-in potential and complete depletion of the nanowire across its diameter and all along its length. Similarly, a reduction in the doping level leads to a reduction in the built-in potential which is much more pronounced compared to the case of the bulk p–n junction. In order to relax doping requirements and improve the properties of the p–n junction such as series resistance, it is necessary to grow nanowires with diameters of a few hundreds of nanometres.

References

[1] Roest A L *et al* 2006 *Nanotechnology* **17** S271
[2] Lensch-Falk J L *et al* 2007 *J. Am. Chem. Soc.* **129** 10670
[3] Calarco R *et al* 2007 *Nano Lett.* **7** 2248
[4] Cui Y and Lieber C M 2001 *Science* **291** 851
[5] Wu Y, Fan R and Yang P 2002 *Nano Lett.* **2** 83
[6] Hiruma K, Yazawa M and Kakibayashi T 1995 *J. Appl. Phys.* **77** 447
[7] Duan X, Huang Y, Cui Y, Wang J and Lieber C M 2001 *Nature* **409** 66
[8] Björk M T *et al* 2002 *Appl. Phys. Lett.* **80** 1058
[9] Huang Y, Duan X, Cui Y and Lieber C M 2002 *Nano Lett.* **2** 101
[10] Solanki R, Huo J, Freeouf J L and Miner B 2002 *Appl. Phys. Lett* **81** 3864
[11] Björk M T *et al* 2002 *Appl. Phys. Lett.* **81** 4458
[12] Zhong Z, Qian F, Wang D and Lieber C M 2003 *Nano Lett.* **3** 343
[13] Kamat P V 2007 *J. Phys. Chem.* C **111** 2834
[14] Soci G *et al* 2007 *Nano Lett.* **7** 1004
[15] Tian B *et al* 2007 *Nature* **449** 885
[16] Agarwal P *et al* 2007 *Nano Lett.* **7** 896
[17] Tutuc E *et al* 2006 *Nano Lett.* **6** 2070
[18] Hu J *et al* 2007 *Proc. SPIE* **6468** 64681E-1
[19] Kayes B M, Atwater H A and Lewis N S 2005 *J. Appl. Phys.* **97** 114302
[20] Zervos M and Feiner L F 2004 *J. Appl. Phys.* **95** 281
[21] Trellakis A *et al* 1997 *J. Appl. Phys.* **81** 7880
[22] Leonard F and Talin A A 2006 *Phys. Rev. Lett.* **97** 026804
[23] Hang Q *et al* 2007 *Appl. Phys. Lett.* **90** 062108
[24] Persson M P and Xu H Q 2006 *Phys. Rev.* B **73** 035328
[25] Lew Yan Voon L C, Lassen B, Melnik R and Willatzen M 2004 *J. Appl. Phys.* **96** 4660